author preprint 2023; to appear in IEEE Transactions on Power Systems DOI: 10.1109/TPWRS.2023.3305093

Risk Assessment and Mitigation of Cascading Failures Using Critical Line Sensitivities

Yitian Dai, *Student Member, IEEE*, Matthias Noebels, Robin Preece, *Senior Member, IEEE*, Mathaios Panteli, *Senior Member, IEEE*, and Ian Dobson, *Fellow, IEEE*

***Abstract*—Security concerns have been raised about cascading failure risks in evolving power grids. This paper reveals, for the first time, that the risk of cascading failures can be increased at low network demand levels when considering security-constrained generation dispatch. This occurs because critical transmission corridors become very highly loaded due to the presence of centralized generation dispatch, e.g., large thermal plants far from demand centers. This increased cascading risk is revealed in this work by incorporating security-constrained generation dispatch into the risk assessment and mitigation of cascading failures. A security-constrained AC optimal power flow, which considers economic functions and security constraints (e.g., network constraints, $N-1$ security, and generation margin), is used to provide a representative day-ahead operational plan. Cascading failures are simulated using two simulators, a quasi-steady state DC power flow model, and a dynamic model incorporating all frequency-related dynamics, to allow for result comparison and verification. The risk assessment procedure is illustrated using synthetic networks of 200 and 2,000 buses. Further, a novel preventive mitigation measure is proposed to first identify critical lines, whose failures are likely to trigger cascading failures, and then to limit power flow through these critical lines during dispatch. Results show that shifting power equivalent to 1% of total demand from critical lines to other lines can reduce cascading risk by up to 80%.**

***Index Terms*—Cascading failure, frequency stability, power generation dispatch, risk assessment.**

I. Introduction

CASCADING failures are recognized as the main cause of large blackouts [1]. Large blackouts, although they rarely occur, have significant social and economic impacts. As a result, risk assessment of cascading failure has long been required by NERC reliability standards to facilitate decision making and investment planning [2].

As summarized in [3], methods for cascading failure risk assessment are mainly based on cascading simulations and statistical analysis of utility outage data. Standard metrics, such as Expected Demand Not Supplied (EDNS), are produced to quantify the resulting impact of cascading failures. This allows benchmarking of various cascading failure simulators and evaluating changes in cascading risk over slow system evolution. Previous studies have shown that cascading risk does not increase proportionally with network loading. Instead, there is a critical loading at which the cascading risk rises sharply and the probability distribution of demand losses exhibits a power-law dependence, indicating an increased risk of large-scale outages [4]–[6]. The power-law dependence of outage probability on outage size is expressed in the form $Pr \sim X^{\alpha}$, where X is the amount of demand loss, and α is the power-law exponent and slope when using logarithmic axes. However, these studies were performed using a proportional dispatch method to schedule generation at different loading levels. That is, changes in demand are proportionally distributed to all available generators, regardless of cost. To improve this, the authors in [7] computed generation dispatch for each loading level using a security-constrained DC optimal power flow, but its impact on cascading risk quantification has not been adequately investigated. Work remains to study the relationship between generation dispatch considerations and cascading risk assessment to inform system planning and operational decisions.

Mitigation measures of cascading failures have been investigated by several researchers, such as in [7]–[12]. A discussion of the challenges of developing measures for cascading failures mitigation, and the learned lessons of deploying such measures can be found in [11]. Existing measures mitigate cascading outages mainly by: 1) identifying and strengthening critical assets [7]–[9], 2) scheduling system resources (e.g., backup generation and synchronous condensers) during planning and operational processes [8], [12], or 3) deploying intentional islanding techniques [10]. These mitigation measures are often based on a given power system model, identifying critical assets and supporting system operators in deciding when to apply the measure. Extensive simulation and detailed cascading failure models are required to thoroughly test their effectiveness.

Applications of generation dispatch techniques in cascading risk estimation and mitigation are less well explored [3], for several reasons. First, the modelling of cascading failures remains a complicated problem. Existing cascading failure simulators can only capture a subset of cascading mechanisms based on different research objectives. Without a systematic validation procedure, the information obtained from dispatch techniques may vary depending on different modelling assumptions [13]. Second, it is challenging to provide reliable estimations of expected costs associated with generation dispatch, control actions and power outages. Uncertainties arise from the operating

This work was supported by the EPSRC Centre for Doctoral Training in Power Networks (EP/L016141/1) and USA NSF grant 1735354.

Y. Dai, M. Noebels and R. Preece are with The University of Manchester, Manchester M13 9PL, UK (emails: {yitian.dai; matthias.noebels; robin.preece}@manchester.ac.uk).

M. Panteli is with the University of Cyprus, Nicosia 1678, Cyprus (e-mail: panteli.mathaios@ucy.ac.cy).

I. Dobson is with the Iowa State University, Ames IA 50011-2140, USA (e-mail: dobson@iastate.edu).

state, the occurrence of certain contingencies, the system operator's behaviors, etc. Making optimal decisions under uncertainty requires a trade-off between the solution quality, the provision of probabilistic guarantees and the computational tractability. Modelling assumptions need to be carefully identified and validated against the limited knowledge available at the time of decision making. This gives rise to a range of different programming formulations, including stochastic optimization [14] and two-stage robust optimization [15]. Given the computational burden, applications of these optimization theories often rely on simplified approximations of post-contingency states and the use of a DC power flow model, and show limitations in providing realistic and usable dispatch solutions for cascading risk management. If not combined with detailed modelling of system dynamics, the optimization problem can lead to overly conservative decisions, and it is difficult to validate optimal solutions under different operating conditions [15].

Security-constrained optimal power flow (SCOPF) is a powerful scheduling tool for power system operators for day-ahead operational planning. SCOPF aims at minimizing the operational cost while satisfying network constraints under normal and contingency operations [16]. The formulation of SCOPF problems considers various control actions, mainly divided into preventive (i.e., pre-contingency) [17] and corrective (i.e., post-contingency) [18] control actions. The state-of-the-art methodologies and challenges for solving SCOPF problems are discussed in [19]. Most existing SCOPF studies focus on managing control strategies and optimizing mathematical programming to deal with failure events that lead to small-scale violations. In many cases, these violations can be eliminated in subsequent cascades without causing a major power outage (e.g., a small-scale cascade caused by a single component failure). However, the nature of cascading failures has led to the widely observed power-law distribution of demand losses [4]. This suggests that certain combinations of events can trigger high-impact cascading failures, although they occur with relatively low probability. Thus, research on small-scale violations is not sufficient in characterizing cascading phenomena, and the coupling of SCOPF with cascading failure simulation has not been adequately investigated.

To address these limitations, this paper incorporates security-constrained AC optimal power flow (SC-ACOPF) into the risk assessment and mitigation of cascading failures. The use of SC-ACOPF provides a day-ahead generation dispatch solution, prioritizing cheaper generation technologies, and ensuring that network constraints and $N-1$ security are respected. It therefore provides insights into the interactions of dispatch considerations with blackout risk, and the potential improvement that preventive operational measures can make on cascading risk mitigation. The proposed preventive SC-ACOPF mitigates cascading risk by limiting the power flow through critical lines, whose tripping could lead to cascading failures. A *Risk Sensitivity Index* (*RSI*) is computed to reveal the sensitivity of cascading risk to individual line loading, and to identify critical lines where constraining power flow can reduce cascading risk. Then, the *RSI* values are used as weight factors for each line, and additional power flow constraints are imposed on critical lines to enhance the reliability of the power system against cascading failures. In particular, this paper:

- makes the first quantification of increased cascading risk at lower demand levels when using SC-ACOPF instead of the proportional dispatch method.
- integrates dispatch considerations and frequency dynamics into cascading failure simulation and risk assessment.
- shows that assuming proportional dispatch can underestimate cascading risk.
- mitigates cascading risk by computing risk sensitivity indexes and constraining power flow on the critical lines.
- coordinates quasi-steady state and dynamic simulation for more robust and practical cascading risk assessment.

The rest of this paper proceeds as follows: Section II begins with the formulation of SC-ACOPF problem. Then, methods for risk assessment and blackout mitigation are described. Section III describes the static and dynamic cascading failure simulators. Simulation results are presented in Section IV for the 200-bus and 2,000-bus systems to illustrate the impact of dispatch factors and the performance of mitigation measures using critical line sensitivities. Section V concludes the paper.

II. Risk Assessment and Mitigation Procedures

Fig. 1 illustrates the cascading failure risk assessment and mitigation procedures with security-constrained dispatch considerations. This framework begins with a SC-ACOPF solution, which offers a representative day-ahead operational plan. In contrast to the proportional generation dispatch commonly used in cascading failure analysis, SC-ACOPF provides valuable insights into the advantages gained by implementing efficient dispatch solutions. Following this, the framework proceeds with generic procedures for cascading failure simulation, risk assessment, and blackout mitigation to evaluate the current security state against expected but not yet occurring contingencies and implement effective mitigation measures. The following subsections describe the three main parts required to apply this approach: (A) obtaining the cheapest pre-contingency dispatch, while ensuring system availability in steady-state and under all $N-1$ contingencies for a system with N lines, (B) risk assessment of cascading failures under $N-k$ contingencies (for cascading failures initiated by k line outages, where k can be in the order of $\{2, 3, 4, \dots\}$), and (C) determining and applying preventive operational measure to find the re-dispatch solution.

A. Formulation of SC-ACOPF Problem

The conventional formulation of the SCOPF problem is adopted from [17], [18] and compactly expressed as follows.

$$\min f(x_0, u_0) \tag{1}$$

$$\text{s.t.} \quad g_0(x_0, u_0) = 0 \tag{2}$$

$$h_0(x_0, u_0) \leq 0 \tag{3}$$

$$g_n(x_n, u_n) = 0 \qquad n = \{1, 2, \dots, c\} \tag{4}$$

$$h_n(x_n, u_n) \leq 0 \qquad n = \{1, 2, \dots, c\} \tag{5}$$

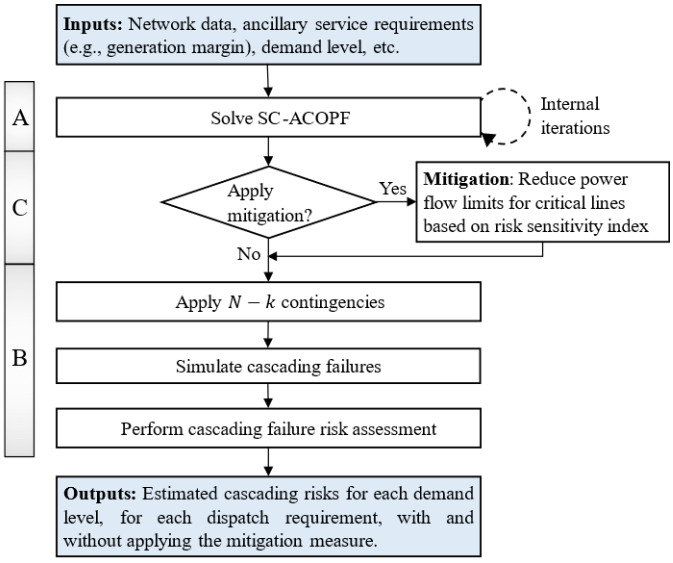

Fig. 1: Flowchart of cascading failures risk assessment and mitigation procedures with security-constrained dispatch considerations.

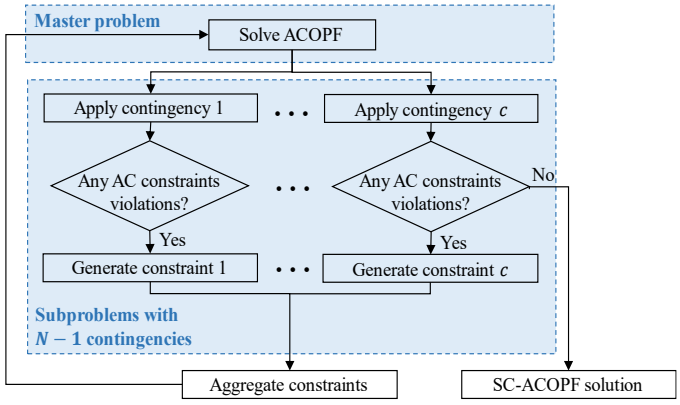

Fig. 2: Flowchart to solve SC-ACOPF with Benders decomposition.

In (1), $f(x_0, u_0)$ is the objective function of system state variable vector x, and control variable vector u. Subscript $n = \{1, 2, \dots, c\}$ denotes variables and constraints associated with the n-th contingency ($n = 0$ refers to the pre-contingency system configuration). x_n is the vector of state variables, i.e., bus voltage magnitudes and phase angles. u_n is the vector of control variables, such as generator real power, generator terminal voltages, and transformer tap settings. This paper focuses on the preventive capabilities in pre-contingency states (e.g., generator frequency control, automatic tap-changers, etc.) and does not consider post-contingency corrective actions, i.e., $u_n = u_0, \forall\, n = \{1, 2, \dots, c\}$. More details on the corrective SCOPF problem can be found for instance in [20]–[22].

Constraints (2, 3) and (4, 5) ensure the reliability of the pre-contingency and post-contingency states, respectively. Equality constraints (2, 4) define the AC power flow equations. Inequality constraints (3, 5) include physical limits on device loading. Among the various types that may be enforced, this procedure imposes constraints on generator active power outputs, power flow through each line/transformer, bus voltages, and overall generation margin. Here, generation margin of generator i is defined as its excessive generation capacity, i.e., difference between maximum and actual active power generation, as shown in (6). The overall generation margin is enforced to be close to a certain amount M (in MW), as shown in (7) where U_i is the state (on=1 and off=0) of generator i, and N_G is the number of available generators. Due to the discrete nature of generator capacity, the expected generation margin is set with the tolerance of the minimum unit capacity, i.e., $\min_i\{P_i\}$.

$$M_i = P_i^{max} - P_i \tag{6}$$

$$M - \min_i\{P_i\} \le \sum_{i=1}^{N_G} U_i M_i \le M + \min_i\{P_i\} \tag{7}$$

$N-1$ security is achieved via an iterative process, starting with a dispatch solution, testing all single line outages, imposing additional power flow constraints, and computing the new SC-ACOPF solution iteratively until no single failure will lead to further outages. Previous studies have shown that the computation time of standard SC-ACOPF grows quadratically with the number of contingencies, but can be reduced to linear growth by Benders decomposition [23], [24]. This is an efficient method of decomposing an optimization problem into a master problem and subproblems. As shown in Fig. 2, the master problem aims to minimize the operational cost under normal operation. Control variables are then sent to subproblems to see if there are any violations under each $N-1$ contingency. In case that the dispatch solution to the master problem does not satisfy the operational constraints for a specific contingency, additional constraints are generated that force the relevant control variables to be within limits for the next iteration, thus making the subproblem feasible. For example, if some lines become overloaded due to a single line outage, then additional power flow constraints are imposed on each violated line as shown in (8), where e_{ij} represents the power flow change of line i (in MVA) caused by the outage of line j, and F_i and F_i^{max} are the pre-contingency power flow and short-term emergency rating of line i, respectively. This process for $N-1$ security check is repeated until the solution to the master problem satisfies the constraints for all sub-problems.

$$-F_i^{max} \le F_i + e_{ij} \le F_i^{max} \tag{8}$$

B. Risk Assessment of Cascading Failures

The cascading risk of a failure scenario is quantified by its probability and impact [3]. Given a set of all possible failure scenarios Ω, the cascading risk ($R(x)$) at a particular state x can be estimated as (9), where $P(c)$ and $I(c, x)$ are the probability and impact of failure scenario c. In this study, the impact of a failure scenario refers to the blackout size in MW measured by the cascading failure models (described in Section III). These models are designed to simulate various disturbances that could initiate a cascading failure, capture the dynamics and propagation of cascading outages and calculate the resulting demand loss. Therefore, $R(x)$ can be interpreted as the expected value of $I(c, x)$ in MW. Considering that it may not be feasible to

simulate all possible failure scenarios, a subset of scenarios (Ω_s) is randomly sampled from Ω according to the probability function $P(c)$. That is, scenarios are weighted according to their probability of occurrence, and scenarios with higher probability are more likely to appear in the sampling set. The estimated risk $\hat{R}(x)$ is given as (10), where $|\Omega|$ and $|\Omega_s|$ represent the number of samples in Ω and Ω_s, respectively. It is clear that $\hat{R}(x)$ converges to $R(x)$ when $|\Omega_s| \to |\Omega|$. To obtain unbiased results, Ω_s needs to be carefully determined, so that it provides an adequate and representative subset of Ω, covering a wide range of probabilities and impacts of failure scenarios.

$$R(x) = \sum_{c \in \Omega} P(c) I(c, x) \tag{9}$$

$$\hat{R}(x) = \frac{|\Omega|}{|\Omega_s|} \sum_{c \in \Omega_s} P(c) I(c, x) \tag{10}$$

The focus of this work is to estimate the risk of cascading failures initiated by simultaneous failures of k lines, i.e., to perform an $N-k$ contingency cascading analysis for a system with N lines. Specifically, if the system has N lines and the sequence of failures is ignored, Ω_k represents the subset of Ω, where k simultaneous line outages start the simulation of cascading failures. This contains $|\Omega_k| = \frac{N!}{k!(N-k)!}$ failure scenarios for a complete $N-k$ analysis. Moreover, it is assumed that the initial outages in each scenario are independent, i.e., the probability of an initial event is the product of the individual outage probabilities. Correlations between initial outages, such as aging degree [25] and spatial correlation [26], [27] have been already investigated in some studies. Such factors can be applied if desired without affecting the general methodology presented here.

The infrequent outages and sparse outage data hinder practical risk assessment in cascading failure analysis. Existing methods for estimating transmission line failure probabilities include: 1) considering common line features like length, location, and proximity [28], 2) utilizing fragility curves to map failure probabilities to weather profiles within each weather region [29], and 3) performing statistical analysis of utility outage data to determine failure rates [30], [31]. Among all estimation methods, line length plays a role in determining the line outage rates against extreme events. Indeed, transmission line outage rates are often expressed per mile or per kilometer [28], [31], [32]. Here, following [28], [31], the failure probability of each line is assumed to be proportional to its length and impedance, given a consistent impedance per unit length. It is important to note that this assumption may not be appropriate for extreme line lengths or extreme weather intensities [31]. In cases where amply sufficient line outage data is available, a more detailed probability distribution of line failure can be utilized, allowing for a more nuanced analysis without altering the general methodology presented. Therefore, the failure probability of each line is assigned according to the line impedance. As shown in (11), the initial probability of a failure scenario c as an $N-k$ contingency can be estimated to be proportional to the product of k line impedances (Z_l). Equation (12) represents the total initial probability of all $N-k$ contingencies. Then, all failure probabilities are normalized so that the total probability of all possible $N-k$ scenarios is equal to the probability (λ_k) of an $N-k$ contingency occurring in the next simulation step, where k can be in the order of $\{2, 3, 4, \ldots\}$. The normalized probability of each $N-k$ contingency can be expressed as (13), the sum of which equals to λ_k. The total blackout risk caused by $N-k$ contingencies can be estimated as (14), where $\Omega_{k,s}$ is a subset of scenarios randomly sampled from Ω_k according to the probability function $\hat{P}_{norm,k}(c)$.

$$\hat{P}_{ini,k}(c) = \prod_{l \in c} Z_l \tag{11}$$

$$\hat{P}_{ini,k} = \sum_{c \in \Omega_k} \hat{P}_{ini,k}(c) \tag{12}$$

$$\hat{P}_{norm,k}(c) = \frac{\lambda_k \hat{P}_{ini,k}(c)}{\hat{P}_{ini,k}} \tag{13}$$

$$\hat{R}_k(x) = \frac{|\Omega_k|}{|\Omega_{k,s}|} \sum_{c \in \Omega_{k,s}} \hat{P}_{norm,k}(c) I(c, x) \tag{14}$$

C. Approach for Cascading Risk Mitigation

As mentioned in the introduction, by considering security-constrained generation dispatch, this work shows that increased risk can be observed at lower demand levels. This is due to the heavy loading in certain transmission corridors, which will be discussed in Section IV-B where the results are presented. To mitigate the increased cascading risk, a preventive operational measure is proposed to constrain the steady-state transmission limits on critical lines. This can reduce the heavy loading of critical lines and mitigate the propagation severity of cascading failures caused by such critical line failures. As a preventive measure, this mitigation is applied to reduce the probability of cascading phenomena by temporarily reducing the power flow constraints and re-dispatching generation before disturbances cause severe outages. To do so requires information such as network branch connectivity, power flows and load conditions, which can be gathered in reality by leveraging advanced monitoring capabilities without additional investments in electrical infrastructure reinforcement and hardening actions. Full observability of network topology, demand distribution and power flow can be augmented by placing phasor measurement units (PMU) throughout the network [33]. Assuming the PMU measurements are always available for the application, the reported data is then transmitted to a central controller to assess the current security state against expected but not yet occurring contingencies.

A sensitivity analysis is performed to investigate the impact of individual line loading on cascading risk. In order to constrain the power flow through each line individually, a *Risk Sensitivity Index* (*RSI*) vector can be computed to indicate the change in cascading risk when the power flow limit of line i reduces from F_i^{max} to F_i^{limit}, as shown in (15) and (16). That is, the power flow constraint during the sensitivity analysis is

set to be ΔF_i lower than the power flowing through the line in an unconstrained manner. Cascading risks can be estimated based on (14). To establish a fair comparison, the degree of power flow restriction needs to be consistent across all lines, thus for a system with N lines, ΔF_i is defined as a fixed amount of power in MVA, $\forall\, i = \{1, 2, \dots, N\}$. That is, the transmission capacity of each line is reduced by the same amount of power and the impact on cascading risk is quantified as $RSI(i)$. In this sensitivity analysis, ΔF_i is chosen to be equal to 1% of total demand, indicating that power equivalent to 1% of total demand is shifted from line i to other lines in the sensitivity analysis.

$$RSI(i) = \hat{R}_k(x;\ |F_i| \le F_i^{max}) - \hat{R}_k\big(x;\ |F_i| \le F_i^{limit}\big) \quad (15)$$

$$\Delta F_i = F_i^{max} - F_i^{limit} \quad (16)$$

Considering factors such as network topology, generation margin, loading condition and failure probability of initial contingencies, *RSI* values need to be accessed for various scenarios where cascading failures may occur. Then, *RSI* values are used to rank the importance of transmission lines in terms of cascading risk mitigation, and serve as a weight factor for each line to design the re-dispatch mitigation scheme. Finally, an effective mitigation can be achieved by first deciding how much power to shift from the top-ranked lines to other lines, and then imposing power flow restrictions on the top-ranked lines to reduce the potential cascading risks associated with their failure. For example, if N_{cri} is a set of critical lines ranked by *RSI*, additional power flow constraints will be imposed on each line $i \in N_{cri}$, in order to shift a total power of ΔF from the top-ranked N_{cri} lines to other lines. The total transferred power ΔF is shared between these critical lines based on their weight factors, i.e., lines with higher *RSI* values are more restricted. The transferred power and the corresponding constrained power flow limit for each critical line are computed based on (17). The simulation procedures of Fig. 1 need to be conducted with and without considering the mitigation measure to determine the contribution of this preventive operational action to the cascading risk mitigation.

$$|F_i| \le F_i^{max} - \Delta F \frac{RSI(i)}{\sum_{i \in N_{cri}} RSI(i)} \qquad i \in N_{cri} \quad (17)$$

Existing sensitivity analysis methods can be divided into local, screening and global sensitivity tests, which exhibit a trade-off between sensitivity accuracy and computational time [34]. Here, a local one-at-a-time method is used to show the sensitivity of cascading risk to individual line loading, where the impact of constrained power flow on cascading risk is linearized through *RSI* values. While slightly more optimized weights for critical lines may exist, more time is needed for day-ahead solutions, and indeed the inaccuracies caused by the small adjustments to power flow (1%-2% of total demand) are small. The linearized sensitivity analysis is considered computationally tractable and effective for day-ahead operational planning, and such linearization assumption has been made previously in other cascading risk mitigation works, such as [7], [8], [35]. Case studies of cascading risk mitigation are discussed in Section IV-C to demonstrate and compare the improvements in system security at different demand levels. However, it is not within the scope of this work to quantify the costs associated with implementing these improvements. If robust economic data is available, methods for balancing security and cascading risks, such as chance constrained programming [36], can be applied as an interesting possible extension of this work.

III. Cascading Failure Simulators

The above-mentioned risk assessment and mitigation procedures are generic and can be applied to any cascading failure simulator that reflects the impact of cascading phenomena resulting from a given set of initial contingencies. For the comparison and verification of the results, cascading failures are simulated based on two typical modelling approaches [37], i.e., the quasi-steady state DC power flow model (herein referred to as a *static* model), and the time-based dynamic model. Both the static and dynamic simulators were developed by the authors and explained in previous publications [38], [39]. In the prior work detailed in [38], the frequency-related cascading phenomena have been illustrated using these two models. The results obtained from extensive comparisons of performance indicators (e.g., the amount of demand loss and the number of line outages) have shown that the two models can produce consistent data distributions, such as the well-observed power-law distribution of demand loss [4]. Cross-validation between these two models has shown their validity and accuracy, thus supporting their potential to provide useful information in different system scenarios. While the prior work focused on estimating cascading risk under one operating condition, this work computes risk assessment among various demand levels, and incorporates more realistic probability distribution of contingencies and SC-ACOPF into cascading risk estimates. For brevity, only key aspects of the simulator implementations will be described in the following subsections.

A. Static Modelling of Cascading Failures

Several models have been developed for power flow-based steady-state analysis, including the OPA model [40], hidden failure model [41], and Manchester model [42]. The static model used in this study is based on the fast dynamic process of the standard OPA model, representing cascading events as discrete transitions. It starts with a SC-ACOPF solution for generation, demand, and power flow. Then, post-contingency states are computed iteratively. To enhance the representation of frequency response during cascading failures and align with the dynamic model, several modifications have been made to the fast dynamic process of the standard OPA mode: (1) overloaded lines are tripped deterministically, while the standard OPA disconnects overloaded lines probabilistically, (2) after network separation, generation is re-dispatched and load is shed in each island individually, assuming that no operator action occurs during cascades and that a new steady state is reached by frequency control, (3) the static model incorporates over-frequency generator tripping schemes, starting from the smallest

unit, as a result of the large generation surplus that typically occurs after network separation, and (4) the static model explicitly considers the flexibility of generator and load during re-dispatch, with a certain ramp rate and limited generator dispatch and load shedding capabilities. In addition, the static model is simulated using the optimal power flow (OPF) solver from MATPOWER [43].

B. Dynamic Modelling of Cascading Failures

The dynamic simulator is implemented based on DIgSILENT PowerFactory 2023 SP3 and MATLAB version 9.14 (R2023a) via the Python application programming interface. It overcomes the limitations of traditional manual system set-up methods, and represents a significant advance in the field of dynamic modelling of cascading failures in realistically sized power networks. The frequency dependence of system components is explicitly simulated, where speed governor and automatic generation control of all synchronous generators are modelled, and a frequency-dependent ZIP load model is used. Wind turbine is modelled using type 3 model, i.e., doubly-fed induction generator. Five types of protection relays are modelled: thermal relays for transmission line protection, under-frequency load shedding relays for emergency frequency containment, under-/over-frequency generator tripping relays for synchronous generator protection, and generator out-of-step relays for synchronization check. Here, it is assumed that all protective relays can correctly remove circuit elements when triggering conditions are met, and the hidden failures in the protection systems are not considered in this work. Studies analyzing hidden failures in protection systems can be found in [41], [44]. The dynamic model focuses on frequency-related cascading phenomenon, and the impacts of other cascading mechanisms (such as voltage violations and reactive power limits) on the cascading risk estimation remain topics for future work. The detailed introduction and source codes of the dynamic cascading failure model are available in [39]. Based on this dynamic model, the impact of step size on various cascading metrics has been investigated in [45]. Results suggest that a step size of 0.1 s can be considered as a good balance between simulation accuracy and efficiency when simulating cascading failures with frequency dynamics and limited renewable penetration and is therefore used here.

IV. Case Study Applications

The proposed framework is illustrated using two large synthetic systems: the Illinois 200-bus system (ACTIVSg200) [46] and the Texas 2,000-bus system (ACTIVSg2000) [46].

A. Simulation Data

The case studies presented in this section focus on estimating cascading risks following a set of $N-2$ contingencies, i.e., cascading failures initiated by simultaneous failures of two transmission lines. A similar study can be applied to higher-order initial contingencies where $k = \{3, 4, \dots\}$. In large power systems, it is computationally infeasible to perform a complete $N-2$ contingency analysis, and an adequate number of failure scenarios is required to obtain an effective risk estimation. The proper size of the sampling set $\Omega_{k,s}$ can be determined via a separate study of how the estimated cascading risk changes with an increasing number of failure scenarios. Fig. 3 shows the results of this study, where 2,000 $N-2$ contingencies are randomly simulated and plotted as separate curves to eliminate any potential bias from the simulation order. Results show that the estimated cascading risk converges to a consistent value when the number of failure scenarios exceeds 1,000. Specifically, in ACTIVSg200 and ACTIVSg2000, the average estimated risk increases by 0.4% and 1.7% respectively, when the number of scenarios increases from 1,000 to 2,000 (doubling the simulation time). Hence, 1,000 $N-2$ contingencies are selected as a reasonable and computationally feasible sampling size for both networks. In fact, the static cascading failure model typically takes a few minutes to simulate 1,000 failure scenarios, using a desktop PC with Intel Core W-2123, 3.60 GHz CPU and 32 GB RAM. However, the dynamic model takes nearly an hour to complete the same simulation for ACTIVSg200 and 5 days for ACTIVSg2000. This can be improved if a better computer source is available, or if contingency screening/sampling techniques are applied. Methods, such as selection of high impact $N-k$ contingencies [47], variance reduction techniques [48], stratified sampling [27], [49], and likely spatial patterns [27], have been developed to assist in the effective sampling of initial contingencies. However, before these methods can be applied, a detailed verification and validation process is required to check the accuracy of the results from multiple test systems, observed data sets and cascading failure simulators, as requested by IEEE PES Working Group on Cascading Failures [37].

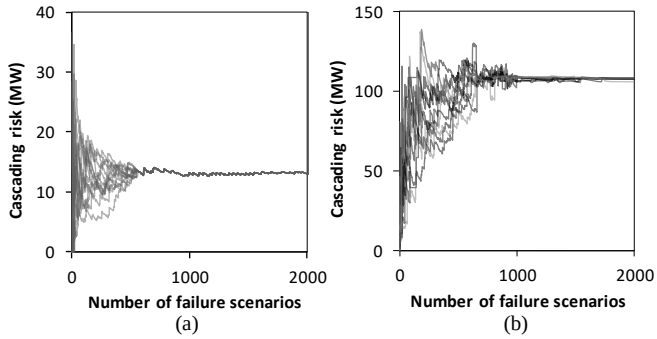

Fig. 3: Dependency of cascading risk on number of failure scenarios using (a) ACTIVSg200 and (b) ACTIVSg2000 systems.

All studies are conducted for the day-ahead operation planning with a simulation period of 24 hours. Reliable data of transmission line failure rate is needed to estimate the probability of an $N-2$ contingency occurring the next day. The daily probability of an $N-2$ contingency is computed based on the transmission line outage data reported by Bonneville Power Administration (BPA) over 10 years [50], which gives the detailed causes and timing of line outages. From 2012 to 2022, 21,001 automatic transmission line outages were recorded. Here, the line outages are grouped into cascades according to the time interval between their occurrences. Assuming that successive outages with a time interval of more than 1 hour belong to different cascades and outages with a time interval of less

than 1 minute occur simultaneously [51], 7,107 cascades are identified, of which 377 cascades are triggered by double line outages (i.e., nearly 0.1 occurrences/day). The BPA transmission network has 688 transmission lines. Considering that a larger network with more transmission lines has a higher probability of double-line outage, the probability (λ_2) of an $N-2$ contingency occurring on the next day is set to 0.1 occurrences/day in ACTIVSg200 and 0.2 occurrences/day in ACTIVSg2000. These probabilities are indicative and can be adjusted if better data is available. The specific probability of each failure scenario can be determined by (13).

To illustrate the impact of different dispatch methods on cascading risk estimation, steady-state operation states at different demand levels are computed using SC-ACOPF and proportional dispatch. 140% and 110% are the highest demand levels for SC-ACOPF convergence to ensure system availability in steady-state and under all $N-1$ contingencies in ACTIVSg200 and ACTIVSg2000, respectively. Thus, in the following simulations, the demand level ranges from 50% to 140% for ACTIVSg200 and 50% to 110% for ACTIVSg2000.

B. *Estimating Risk at Different Demand Levels*

This section first discusses the impact of different dispatch methods and increased generation margin on cascading risk estimation. Then, special attention is paid to the changes in critical transitions as demand increases. In the following discussion, simulations are performed using static and dynamic models to support the validity of the findings. Considering the complexity of the research scope, the application on ACTIVSg200 is mainly used to illustrate the impact of dispatch considerations on cascading risk. The results of ACTIVSg2000 are used to verify the discovery and illustrate the impact of network size.

1) *Proportional Dispatch vs. SC-ACOPF Methods*

This section reveals how the cascading risk varies with the demand level in ACTIVSg200 using both static and dynamic models. The day-ahead operating states are computed using the SC-ACOPF and proportional dispatch methods for comparison. The proportional dispatch method equally distributes the change in demand to all the generators, regardless of cost. In other words, the same set of generators is committed at different demand levels and the generation margin reduces as demand increases. The SC-ACOPF method considers economic factors and system constraints. The setting of generation margin $M = 20\%$ of total demand is first arbitrarily considered, which is in line with industrial practice (e.g., 20-30% in GB [52]). That is, the system always maintains an excess generation capacity equal to 20% of total demand to compensate for large power imbalances. The effect of this assumption is evaluated in Section IV-B-2.

As shown in Fig. 4, the sharp increase at higher demand levels is captured in both simulators and with both dispatch methods. Compared with the static model, the sharp increase of cascading risk occurs at a relatively lower demand level in the dynamic model. This is because the static model ignores the frequency dynamics and tends to underestimate risks, thus leading to a higher level of critical demand. This phenomenon has been previously explored in more detail in [38]. Besides, observed by both simulators, the cascading risk of the proportional dispatch method is much smaller than that of the SC-ACOPF (note the different y-axis scaling). The proportional dispatch assumption allows the generation margin to vary from 350% to 60%, as the demand level increases from 50% to 140%, which is much greater than the 20% generation margin used in SC-ACOPF. This provides a high level of dispatch capability in emergency situations that would not be possible in real power system operation, and results in the significant underestimation of risk. SC-ACOPF considers the dispatch factors such as individual generator output limits and security constraints, but the requirements for these factors need to be carefully determined to achieve an acceptable level of risk.

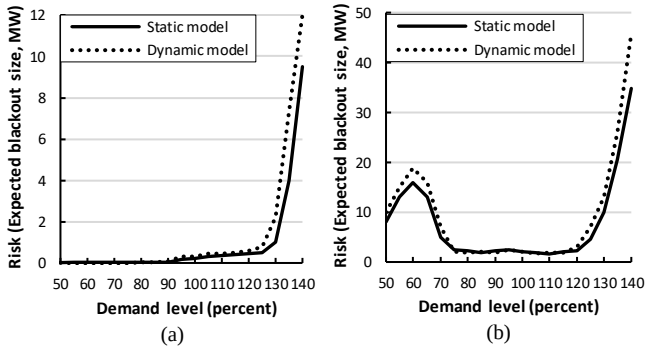

Fig. 4: Cascading failure risk versus demand level in ACTIVSg200 using (a) proportional dispatch and (b) SC-ACOPF. The risks are measured by static and dynamic cascading failure simulators.

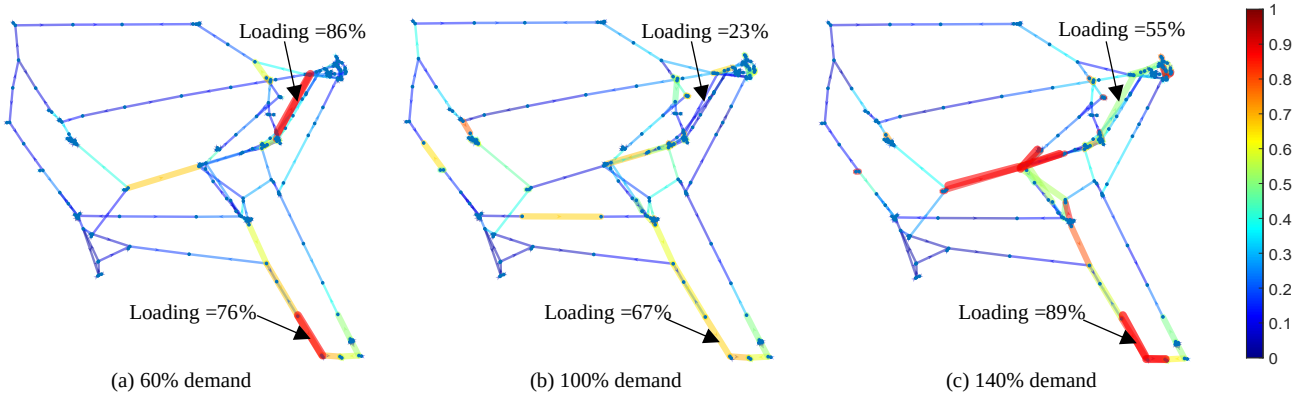

Fig. 5: Heatmaps of line loading conditions for ACTIVSg200 at demand levels of (a) 60%, (b) 100% and (c) 140%, dispatched by SC-ACOPF.

One striking result is that when using SC-ACOPF, the risk does not always increase as the demand increases. In fact, an increased risk is seen at lower demand levels of 50-70%, contrary to the steady growth indicated by the proportional dispatch. This reveals, for the first time, a centralized generation issue in cascading risk management that can happen when the system is operating with a small number of generators. In this case, power from a small number of sources needs to be transmitted to a larger number of load locations, which will lead to a high utilization of a certain part of transmission system to transport the energy from the cheap generation locations. The high utilization of assets will increase the vulnerability of these devices, whose failure will lead to a high risk of cascading failure. To illustrate this, Fig. 5 presents heatmaps of the line loading conditions at three representative demand levels, i.e., 60%, 100% and 140%. Note that the network topology is formed based on line impedances and thus the layout is not geographic. It is shown that at 60% of demand (in Fig. 5(a)), even though the overall system demand level is low, some of lines (as marked) are more utilized than they would be when the demand is 100% (in Fig. 5(b)). In fact, results show that at 60% of demand, cascading failures associated with the top 5 highly utilized lines (as initial event or participating in the cascades) contribute to 42% of the total blackout risk, which result in the increase of blackout risk at lower demand levels. A similar 'bowl-shape' relationship has been observed in [53], indicating that the transition probabilities in a Markov model must change as the cascade proceeds to obtain that power law in cascade size. However, the relationship seen in [53] describes the cascade-stop probability as a function of the progression of failures in a cascade, whereas here the impact of increasing system loading on blackout size is investigated.

2) Impact of the Amount of Generation Margin

In this subsection, the impact of the amount of generation margin (M) on the cascading risk is investigated. This analysis will help to quantify the relationship between increased margin and the resulting system risk. For example, in GB, system operators typically maintain generation margin at 20-30% of total demand [52]. Seasonal reserve margins averaged about 20% for 2021 summer and 25% for 2021-2022 winter across all U.S. regions assessed [54]. Therefore, this study considers M increasing from 10% to 40% with a 10% step size. Fig. 6 shows the extent to which the increased generation margin can mitigate cascading risk in the 200-bus system. It is notable that the results of static and dynamic models show similar trends in cascading risks among various demand levels and generation margin requirements. Whilst differences do exist, among different operating conditions, the dynamic model always provides higher estimated risks than the static model. Dynamic simulation on the 2,000-bus system is time-consuming, as thousands of measurement devices, controllers and relays are simulated concurrently. Considering the high computational cost of the dynamic model and the consistency of results obtained from static and dynamic simulators, the study is conducted on the 2,000-bus network, using only the static simulator to increase computational efficiency as similar trends in cascading risks are observed in the two models. Results are shown in Fig. 7.

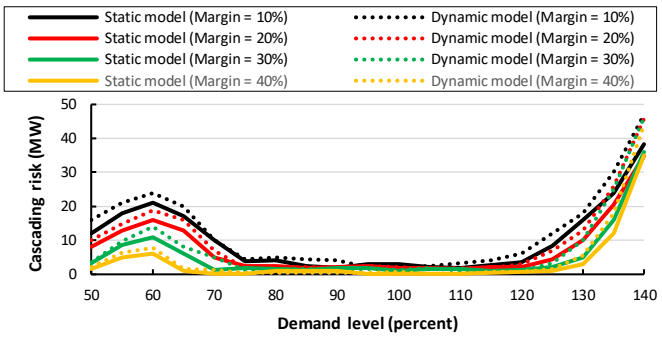

Fig. 6: Dependence of risk on generation margin in ACTIVSg200, using static and dynamic cascading failure simulators.

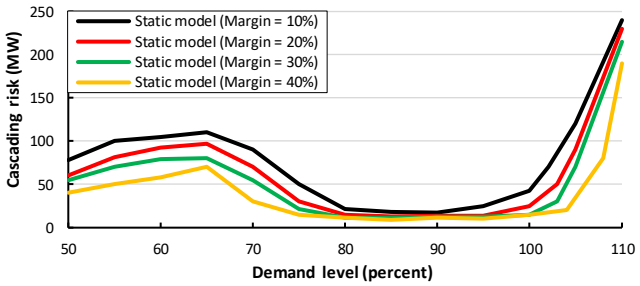

Fig. 7: Dependence of risk on generation margin in ACTIVSg2000, using static cascading failure simulator only.

The increased risk at lower demand levels is reflected in the results of both systems, thus verifying that the centralized generation issue plays an important role in the cascading risk estimation. The increased generation margin can improve generation dispatch capability to compensate large power imbalances and reduce the blackout size. In ACTIVSg200, by increasing the generation margin from 10% to 40%, the risk can be reduced by approximately 78% for demand level below 130%. When the demand level is above 130%, the system is operating under heavily loaded conditions and the contribution of generation margin towards risk reduction is limited. In particular, the cascading risks with different generation margins all converge to a similar value at a demand of 140%. In ACTIVSg2000, increasing generation margin to 40% can reduce the risk by about 40% for demand levels between 50% and 75%, and by about 18% at a demand of 110%. It is expected that further increase in the generation margin can reduce the cascading risk further, but the continuous provision of a large amount of generation margin may not be economically reasonable.

3) Variations in Critical Demand Levels

Existing studies have shown the existence of critical transitions (also referred to as network tipping points or breakpoints) in power systems, as network demand grows. The critical transitions are determined by observing sudden increases in reliability metrics, such as EDNS, the number of component outages and the probability of cascading outages of a certain size [4], [5]. Also, it is widely observed in historical records and simulation-based studies that the probability distribution of cascading risk near the critical demand level is governed by a power-law [1], [4]. The critical transition provides a reference point of system stressing. Recent advances in the field of system stress

testing have emphasized the great potential for detecting near-collapse situations and providing early warning signals by predicting system behavioral changes [55]–[57]. Carefully controlling and operating the power system close to, but below, this critical point can effectively manage cascading risks and ensure economic benefits. This subsection identifies the critical demand levels and power law exponents of ACTIVSg200 and ACTIVSg2000 when using SC-ACOPF, and investigates the probability distribution characteristics of power outages near the critical demand levels.

Here, the critical demand is defined at the point where the gradient of the curves in Fig. 6 and Fig. 7 is greater than 1 MW/percent. Given the similar trends in cascading risks observed between simulation results of static and dynamic simulators, the results of static model are presented here. It can be seen from Table I that the growth in the generation margin slightly increases the critical demand. Systems with higher critical demand levels have greater flexibility to tackle disturbances and gain higher economic benefits by operating at increased levels of transmission system loading without significantly increasing the cascading risk. The exponent of the power law represents the slope of probability density function on a log-log plot, i.e., a smaller absolute value of exponent indicates a slower slope and a heavier tail of the probability distribution. Here, the value of exponent varies from −1.2 to −1.4 and is not sensitive to generation margin or network size. Observing probability distributions of unserved demand with exponents from −1 to −2 is in line with the trends of historical data and results using other cascading failure models [1], [4], [5], which supports the validity of the proposed methodology. However, the correlation between the exponent and disturbance types/network properties has not been examined in previous studies.

TABLE I
CRITICAL DEMAND LEVELS AND APPROXIMATE POWER LAW EXPONENTS WITH DIFFERENT GENERATION MARGINS, DISPATCHED BY SC-ACOPF

	ACTIVSg200				ACTIVSg2000			
Generation margin (%)	10	20	30	40	10	20	30	40
Critical demand (%)	122	124	128	133	102	104	105	107
Power-law exponent	-1.27	-1.25	-1.32	-1.30	-1.25	-1.24	-1.29	-1.34

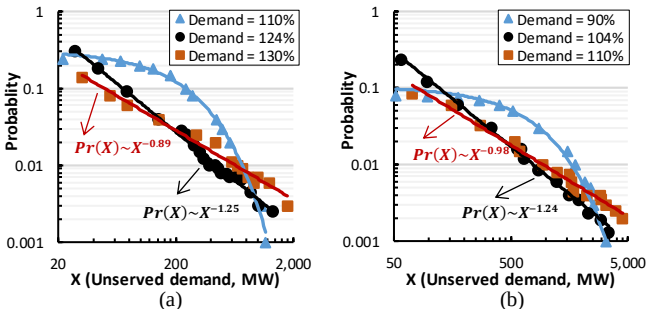

(a) (b)

Fig. 8: Probability density functions of unserved demand for demand levels below (triangles), at (circles) and above (squares) the critical demand with a generation margin of 20% in (a) ACTIVSg200 and (b) ACTIVSg2000.

With a generation margin of 20%, the probability density functions of unserved demand below, at and above the critical demand of ACTIVSg200 and ACTIVSg2000 are shown in Fig. 8. In both systems, the probability distributions of unserved demand below the critical demand show an approximately exponential tail, while the distributions for cases at and above the critical demand show power-law behaviors with different exponents. The power-law tail becomes heavier as demand increases, indicating a higher probability for large blackouts. The critical transition from an exponential tail to a power-law tail of the blackout size is widely reflected in historical data and existing work [4], which highlights the validity of the proposed methodologies and cascading failure simulators. For example, [58] shows the probability distribution of demand loss changing from a lognormal distribution to a regime with a power law tail and then back to a lognormal distribution, as the failure probability of transmission line increases. Fig. 9 of [58] shows a slope change in the power law regime, and this is consistent with the slope changes observed in Fig. 8 here as the demand changes from 124% to 130% in (a), and from 104% to 110% in (b).

C. *Blackout Mitigation*

This section examines the contribution of the proposed mitigation measure to risk reduction. *RSI* values are first computed to provide an importance ranking of transmission lines. Then, targeted preventive measures are developed to reduce transmission stress on critical lines, thus reducing overall cascading risk.

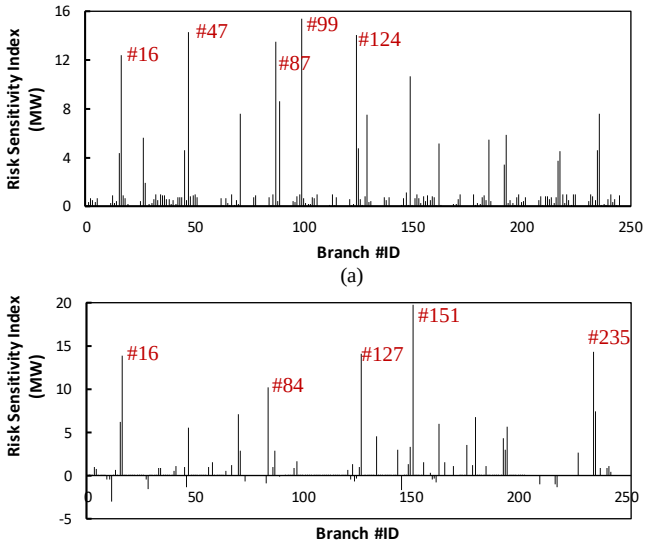

(b)

Fig. 9: Sensitivity of cascading risk to individual line loading for all 245 branches in ACTIVSg200 at demand levels of (a) 60% and (b) 140% with a generation margin of 20% and the dynamic simulator. The five lines with the highest *RSI* values are marked in red.

By reducing line loading individually by an amount equal to 1% of total demand, the sensitivity of cascading risk to individual line loading can be computed from (15). *RSI* values of two typical demand levels (60% and 140%) are shown in Fig. 9, representing high-risk conditions at low and high demand levels. Lines with the highest *RSI* values are marked in red and are targeted for power flow restriction. The ranking of line importance depends on the SC-ACOPF solution and varies with

different levels of demand. At a demand level of 60%, reducing line loading by 1% of total demand (i.e., 9.2 MVA) can reduce the expected cascading risk by up to 15.4 MW, smoothing out the increased risk at this demand level. However, at the 140% demand level, about 5% of lines have negative *RSI* values. This indicates that reducing the loading of these lines does not reduce cascading risk, but rather increases the likelihood of triggering cascading outages when these lines are tripped. This occurs because the system is highly utilized at a high demand level and shifting power from some lines can increase the failure probabilities of other lines, thus increasing the cascading risk.

The proposed mitigation measure imposes additional power flow constraints (as shown in (17)) to avoid the high loading of critical assets. This type of asset high loading can occur, for example, when large-scale offshore wind generation is connected at a single point of common coupling or can be exposed when the system is operating with a small number of generators, as discussed in Section IV-B. Fig. 10 showcases the performance of the proposed mitigation at 60% and 140% demand levels of ACTIVSg200. The ranking of line importance can be read from Fig. 9, for example, the top 5 critical lines at the 60% demand level are $\{99, 47, 124, 87, 16\}$. For each demand level, the cascading risk is evaluated as the total transferred power ΔF increases from 0 to 30 MVA, and N_{cri} increases from including of only the top-ranked line, to including the top-ranked 5 lines, to including all lines. More specifically, study case "1 Line" shifts the transferred power of ΔF from $N_{cri} = \{99\}$ to other lines. Study case "2 Lines" shifts a total power of ΔF from $N_{cri} = \{99, 47\}$ to other lines, where $RSI(99)$=15.4 MW and $RSI(47)$=14.3 MW. ΔF is shared between lines 99 and 47 according to their *RSI* values, i.e., the power flow limits are reduced by 52%ΔF and 48%ΔF for lines 99 and 47 respectively.

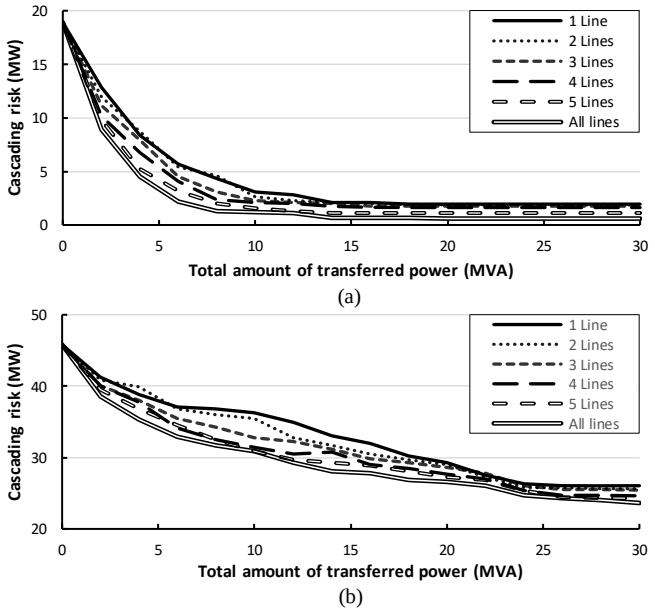

Fig. 10: Dependence of risk on the total amount of transferred power and the number of constrained lines in ACTIVSg200 at demand levels of (a) 60% and (b) 140% with a generation margin of 20% and the dynamic simulator.

The overall trend shows a clear reduction in cascading risk (up to 80%) by deploying the proposed mitigation measure. By constraining the power flow of only the top-ranked 5 lines, a risk reduction comparable to that of constraining all lines can be achieved, with a difference of less than 2% for different values of transferred power. The small difference in results supports the validity of the linearization assumption between cascading risk and individual line loading, which is sufficiently fast to offer a good indication of critical lines for day-ahead operational planning. Specifically, as ΔF increases, cascading risk at the 60% demand level gradually flattens out and the mitigation effect saturates when the total transferred power is above 15 MVA. Furthermore, a steeper slope of risk reduction can be observed as more lines participate in mitigation, but operating at sub-optimal outputs can lead to higher system operation costs. These factors will need to be balanced when optimizing the mitigation of cascading risk. For the demand level of 140%, shifting 30 MVA from the top 5 critical lines to other lines can mitigate cascading risk by 50% but is still around 25 MW. Continuing to limit line loading at this point may not be appropriate for risk mitigation at high demand levels, as the network is already highly utilized. The impact of other dispatch considerations, such as the spatial distribution of generation margin, against blackout mitigation can be further evaluated, so that advances can be made in understanding the relative importance of dispatch considerations under different system conditions.

V. Conclusions

This paper has revealed, for the first time, that an increased risk can be observed at lower demand levels, when security-constrained generation dispatch is considered. This suggests that the presence of readily dispatched centralized generation can lead to high utilization of critical assets and result in a higher risk of power outages. This finding was revealed by incorporating security-constrained AC optimal power flow (SC-ACOPF) into risk assessment and mitigation of cascading failures in power systems. Results showed that the proportional dispatch commonly assumed in cascading failure simulation can underestimate the cascading risk compared to SC-ACOPF dispatch. In addition, based on SC-ACOPF, a novel mitigation measure was proposed to limit critical line loading in the preventive mode and reduce the associated probabilities of line outages during cascading failures.

Two cascading failure simulators were used for result verification: a quasi-steady state DC power flow model and a time-based dynamic model incorporating all frequency dynamics. The proposed approach was illustrated through risk assessment of cascading failures on two large synthetic networks: ACTIVSg200 and ACTIVSg2000. Cascading risks at different demand levels were quantified and the probability distribution characteristics of demand loss near the critical demand levels were investigated. Consistent conclusions were drawn from simulations conducted with two distinct simulators, two large-scale test systems and considering different system settings such as demand levels, generation margins, and power flow constraints. When using SC-ACOPF, an increased cascading risk was observed at low demand levels. Generally, the static

simulator can reflect important information regarding the variation trends of estimated risk but tends to underestimate the cascading risk compared to the dynamic simulator. In addition, increasing generation margin can effectively mitigate cascading risk and push the critical demand to a higher value, but continuously providing a large generation margin solely to prevent occasional power outages may not be economically justified. Furthermore, a *Risk Sensitivity Index* (*RSI*) was defined to describe the sensitivity of cascading risk to individual line loading. The proposed mitigation measure – imposing additional power flow constraints based on *RSI* values – can effectively solve issues associated with heavily loaded assets triggering cascading failures. Case studies of cascading risk mitigation at low and high demand levels provided insights on the contribution of preventive measures on blackout mitigation at different system stressing conditions. In particular, targeted line loading reduction based on *RSI* can mitigate cascading risk almost as effectively as reducing all line loading limits. All these findings emphasized the importance of taking the dispatch considerations into account when performing cascading failure analysis, and carefully formulating these requirements in cascading risk management.

REFERENCES

[1] B. A. Carreras, D. E. Newman, and I. Dobson, "North American Blackout Time Series Statistics and Implications for Blackout Risk," *IEEE Trans. Power Syst.*, vol. 31, no. 6, pp. 4406–4414, 2016.

[2] *Transmission Operations*, NERC Std. TOP-004-2, 2007.

[3] M. Vaiman *et al.*, "Risk assessment of cascading outages: Methodologies and challenges," *IEEE Trans. Power Syst.*, vol. 27, no. 2, pp. 631–641, 2012.

[4] I. Dobson, B. A. Carreras, V. E. Lynch, and D. E. Newman, "Complex systems analysis of series of blackouts: Cascading failure, critical points, and self-organization," *Chaos*, vol. 17, no. 2, 2007.

[5] D. P. Nedic, I. Dobson, D. S. Kirschen, B. A. Carreras, and V. E. Lynch, "Criticality in a cascading failure blackout model," *Int. J. Electr. Power Energy Syst.*, vol. 28, no. 9 SPEC. ISS., 2006.

[6] S. Mei, Y. Ni, G. Wang, and S. Wu, "A study of self-organized criticality of power system under cascading failures based on AC-OPF with voltage stability margin," *IEEE Trans. Power Syst.*, vol. 23, no. 4, pp. 1719–1726, 2008.

[7] P. Rezaei, P. D. H. Hines, and M. J. Eppstein, "Estimating Cascading Failure Risk With Random Chemistry," *IEEE Trans. Power Syst.*, vol. 30, no. 5, pp. 2726–2735, 2015.

[8] B. A. Carreras, V. E. Lynch, D. E. Newman, and I. Dobson, "Blackout mitigation assessment in power transmission systems," *Proc. 36th Annu. Hawaii Int. Conf. Syst. Sci. HICSS 2003*, 2003.

[9] K. Zhou, I. Dobson, Z. Wang, A. Roitershtein, and A. P. Ghosh, "A Markovian Influence Graph Formed from Utility Line Outage Data to Mitigate Large Cascades," *IEEE Trans. Power Syst.*, vol. 35, no. 4, pp. 3224–3235, 2020.

[10] J. Quiros-Tortos, P. Demetriou, M. Panteli, E. Kyriakides, and V. Terzija, "Intentional Controlled Islanding and Risk Assessment: A Unified Framework," *IEEE Syst. J.*, vol. 12, no. 4, 2018.

[11] M. Vaiman *et al.*, "Mitigation and prevention of cascading outages: Methodologies and practical applications," in *IEEE Power and Energy Society General Meeting*, 2013.

[12] N. Al Masood, R. Yan, and T. Kumar Saha, "Cascading Contingencies in a Renewable Dominated Power System: Risk of Blackouts and Its Mitigation," *IEEE Power Energy Soc. Gen. Meet.*, 2018.

[13] X. Liu and Z. Li, "Revealing the impact of multiple solutions in DCOPF on the risk assessment of line cascading failure in OPA model," *IEEE Trans. Power Syst.*, vol. 31, no. 5, 2016.

[14] Q. P. Zheng, J. Wang, and A. L. Liu, "Stochastic Optimization for Unit Commitment - A Review," *IEEE Trans. Power Syst.*, vol. 30, no. 4, 2015.

[15] H. Qiu, W. Gu, P. Liu, Q. Sun, Z. Wu, and X. Lu, "Application of two-stage robust optimization theory in power system scheduling under uncertainties: A review and perspective," *Electr. Power Syst. Res.*, 2022.

[16] B. Stott and O. Alsaç, "Optimal power flow–basic requirements for real-life problems and their solutions (White paper)," *SEPOPE XII Symp. Rio Janeiro, Brazil*, 2012.

[17] O. Alsac and B. Stott, "Optimal load flow with steady-state security," *IEEE Trans. Power Appar. Syst.*, no. 3, pp. 745–751, 1974.

[18] A. Monticelli, M. V. F. Pereira, and S. Granville, "Security-Constrained Optimal Power Flow with Post-Contingency Corrective Rescheduling," *IEEE Power Eng. Rev.*, no. 2, pp. 43–44, 1987.

[19] F. Capitanescu *et al.*, "State-of-the-art, challenges, and future trends in security constrained optimal power flow," *Electr. Power Syst. Res.*, vol. 81, no. 8, pp. 1731–1741, 2011.

[20] E. Karangelos and L. Wehenkel, "An Iterative AC-SCOPF Approach Managing the Contingency and Corrective Control Failure Uncertainties with a Probabilistic Guarantee," *IEEE Trans. Power Syst.*, vol. 34, no. 5, 2019.

[21] F. Capitanescu and L. Wehenkel, "Improving the statement of the corrective security-constrained optimal power-flow problem," *IEEE Trans. Power Syst.*, vol. 22, no. 2, 2007.

[22] F. Capitanescu, T. Van Cutsem, and L. Wehenkel, "Coupling optimization and dynamic simulation for preventive-corrective control of voltage instability," *IEEE Trans. Power Syst.*, vol. 24, no. 2, 2009.

[23] Y. Li and J. D. McCalley, "Decomposed SCOPF for improving efficiency," *IEEE Trans. Power Syst.*, vol. 24, no. 1, 2009.

[24] X. Wu and A. J. Conejo, "Security-Constrained ACOPF: Incorporating Worst Contingencies and Discrete Controllers," *IEEE Trans. Power Syst.*, vol. 35, no. 3, 2020.

[25] W. Li, "Incorporating Aging Failures in Power System Reliability Evaluation," *IEEE Power Engineering Review*, vol. 22, no. 7. 2002.

[26] L. A. Clarfeld, P. D. H. Hines, E. M. Hernandez, and M. J. M. Eppstein, "Risk of Cascading Blackouts Given Correlated Component Outages," *IEEE Trans. Netw. Sci. Eng.*, 2020.

[27] K. Zhou, I. Dobson, and Z. Wang, "The Most Frequent N-K Line Outages Occur in Motifs That Can Improve Contingency Selection," *IEEE Trans. Power Syst.*, 2023.

[28] A. Moradkhani, M. R. Haghifam, and M. Mohammadzadeh, "Failure rate estimation of overhead electric distribution lines considering data deficiency and population variability," *Int. Trans. Electr. Energy Syst.*, vol. 25, no. 8, 2015.

[29] M. Panteli, D. N. Trakas, S. S. Member, P. Mancarella, S. S. Member, and N. D. Hatziargyriou, "Boosting the Power Grid Resilience to Extreme Weather Events Using Defensive Islanding," *IEEE Trans. Smart Grid*, vol. 7, no. 6, pp. 2913–2922, 2016.

[30] K. Zhou *et al.*, "Bayesian Estimates of Transmission Line Outage Rates That Consider Line Dependencies," *IEEE Trans. Power Syst.*, vol. 36, no. 2, pp. 1095–1106, 2021.

[31] T. Iešmantas and R. Alzbutas, "Bayesian spatial reliability model for power transmission network lines," *Electr. Power Syst. Res.*, vol. 173, 2019.

[32] S. Ekisheva, R. G. Bauer, M. Lauby, and B. D. Till, "Reliability indices and performance statistics for transmission elements of the North American bulk power system," *2018 Int. Conf. Probabilistic Methods Appl. to Power Syst. PMAPS 2018 - Proc.*, 2018.

[33] A. Asgari and K. G. Firouzjah, "Optimal PMU placement for power system observability considering network expansion and N-1 contingencies," *IET Gener. Transm. Distrib.*, vol. 12, no. 18, 2018.

[34] A. Saltelli et al., *Global sensitivity analysis: The primer*. Wiley, 2008

[35] J. Qi, "Utility Outage Data Driven Interaction Networks for Cascading Failure Analysis and Mitigation," *IEEE Trans. Power Syst.*, vol. 36, no. 2, pp. 1409–1418, 2021.

[36] H. Wu, M. Shahidehpour, Z. Li, and W. Tian, "Chance-constrained day-ahead scheduling in stochastic power system operation," *IEEE Trans. Power Syst.*, vol. 29, no. 4, 2014.

[37] J. Bialek *et al.*, "Benchmarking and Validation of Cascading Failure Analysis Tools," *IEEE Trans. Power Syst.*, vol. 31, no. 6, pp. 4887–4900, 2016.

[38] Y. Dai, M. Noebels, M. Panteli, and R. Preece, "Evaluating the Effect of Dynamic and Static Modelling on Cascading Failure Analysis in Power Systems," in *2021 IEEE Madrid PowerTech*, 2021.

[39] Y. Dai, M. Panteli, and R. Preece, "Python Scripting for DIgSILENT PowerFactory: Enhancing Dynamic Modelling of Cascading Failures," in *2021 IEEE Madrid PowerTech*, 2021.

[40] B. A. Carreras, D. E. Newman, I. Dobson, and N. S. Degala, "Validating OPA with WECC data," *46th Hawaii International Conference on System Sciences*, 2013.

[41] J. Chen, J. S. Thorp, and I. Dobson, "Cascading dynamics and mitigation assessment in power system disturbances via a hidden failure model," *Int. J. Electr. Power Energy Syst.*, 2005.

[42] M. A. Rios, D. S. Kirschen, D. Jayaweera, D. P. Nedic, and R. N. Allan, "Value of Security: Modeling Time-Dependent Phenomena and Weather Conditions," *IEEE Power Eng. Rev.*, vol. 22, no. 7, p. 53, 2002.

[43] R. D. Zimmerman, C. E. Murillo-Sanchez, and R. J. Thomas, "MATPOWER: Steady-State Operations, Planning, and Analysis Tools for Power Systems Research and Education," *IEEE Trans. Power Syst.*, vol. 26, no. 1, pp. 12–19, 2011.

[44] A. G. Phadke and J. S. Thorp, "Expose hidden failures to prevent cascading outages," *IEEE Comput. Appl. Power*, vol. 9, no. 3, 1996.

[45] Y. Dai, M. Noebels, M. Panteli, and R. Preece, "Benefits and Challenges of Dynamic Modelling of Cascading Failures in Power Systems," in *11th Bulk Power Systems Dynamics and Control Symposium (IREP 2022)*, 2022.

[46] A. B. Birchfield, T. Xu, K. M. Gegner, K. S. Shetye, and T. J. Overbye, "Grid Structural Characteristics as Validation Criteria for Synthetic Networks," *IEEE Trans. Power Syst.*, vol. 32, no. 4, 2017.

[47] M. J. Eppstein and P. D. Hines, "A 'random chemistry' algorithm for identifying collections of multiple contingencies that initiate cascading failure," *IEEE Trans. Power Syst.*, vol. 27, no. 3, pp. 1698–1705, 2012.

[48] J. Guo, F. Liu, J. Wang, J. Lin, and S. Mei, "Toward Efficient Cascading Outage Simulation and Probability Analysis in Power Systems," *IEEE Trans. Power Syst.*, vol. 33, no. 3, 2018.

[49] F. Faghihi, P. Henneaux, and M. Panteli, "An efficient probabilistic approach to dynamic resilience assessment of power systems," *Congrès Lambda Mu 22 «Les risques au cœur des transitions»(e-congrès)-22e Congrès Maîtrise des Risques Sûreté Fonct.*, 2020.

[50] "Bonneville power administration transmission services operations and reliability reports," *BPA*, 2023. [Online]. Available: https://transmission.bpa.gov/Business/Operations/Outages

[51] I. Dobson, "Estimating the propagation and extent of cascading line outages from utility data with a branching process," *IEEE Trans. Power Syst.*, vol. 27, no. 4, pp. 2146–2155, 2012.

[52] National Grid ESO, "Daily Operational Planning Margin Requirement." [Online]. Available: https://data.nationalgrideso.com/generation/daily-opmr/r/daily_operational_planning_margin_requirement.

[53] M. Rahnamay-Naeini and M. M. Hayat, "Impacts of Operating Characteristics on Sensitivity of Power Grids to Cascading Failures.", *IEEE Power and Energy Society General Meeting (PESGM)*, 2016.

[54] NERC, "2022 State of Reliability," [Online]. Available: https://www.nerc.com/pa/RAPA/PA/Performance Analysis DL/NERC_SOR_2022.pdf

[55] H. Ren and D. Watts, "Early warning signals for critical transitions in power systems," *Electr. Power Syst. Res.*, vol. 124, 2015.

[56] M. B. DeMenno, R. J. Broderick, and R. F. Jeffers, "From systemic financial risk to grid resilience: Embedding stress testing in electric utility investment strategies and regulatory processes," *Sustain. Resilient Infrastruct.*, vol. 7, no. 6, pp. 673–694, 2022.

[57] L. Galbusera and G. Giannopoulos, "Leveraging network theory and stress tests to assess interdependencies in critical infrastructures," in *Advanced Sciences and Technologies for Security Applications*, 2019.

[58] B. A. Carreras, J. M. Reynolds-Barredo, I. Dobson, and D. E. Newman, "Critical behavior of power transmission network complex dynamics in the OPA model," *Chaos*, vol. 29, no. 3, 2019.

Yitian Dai (S'21) received the B.Eng. from The University of Manchester, Manchester, U.K, and North China Electric Power University, Hebei, China, in 2018. She is currently working toward the Ph.D. degree with the Department of Electrical and Electronic Engineering, The University of Manchester. Her research interest includes power system dynamics and risk assessment of cascading failures.

Matthias Noebels received the M.Sc. degree in physics from the University of Konstanz, Konstanz, Germany, in 2015, and the Ph.D. degree in electrical engineering with the Centre for Doctoral Training in Power Networks, The University of Manchester, Manchester, U.K., in 2022. His expertise lies in resilience analysis of power networks as well as developing strategies that can enhance resilience in case of natural hazards such as extreme weather.

Robin Preece (M'13–SM'18) received the B.Eng. and Ph.D. degrees from The University of Manchester, Manchester, U.K. He is currently a Reader in Future Power Systems with the Department of Electrical and Electronic Engineering, The University of Manchester, where he has been an academic since July 2014. His research interests focus on the stability and operation of future power systems.

Mathaios Panteli (S'09–M'13–SM'18) received the M.Eng. degree in electrical and computer engineering from Aristotle University of Thessaloniki, Greece, in 2009, and the Ph.D. degree in electrical power engineering from The University of Manchester, U.K., in 2013. He is currently an Assistant Professor with the Department of Electrical and Computer Engineering, University of Cyprus, and an Honorary Lecturer in the Department of Electrical and Electronic Engineering, Imperial College London. His main research interests include techno-economic reliability, resilience and flexibility assessment of future low-carbon energy systems, grid integration of renewable energy sources and integrated modelling and analysis of co-dependent critical infrastructures. Dr Panteli is an IET Chartered Engineer (CEng), the Chair of the CIGRE Working Group C4.47 "Power System Resilience" and the CIGRE Cyprus National Committee, and an active member of multiple IEEE working groups.

Ian Dobson (IEEE Fellow) received the B.A. in mathematics from Cambridge University and the Ph.D. in electrical engineering from Cornell University. He previously worked for British industry and the University of Wisconsin- Madison, and is currently Sandbulte Professor of Electrical Engineering at Iowa State University. His interests are power system resilience, blackout risk, cascading failure, complex systems, and nonlinear dynamics.